On the quality of high-resolution scatterometer winds

Jur Vogelzang,[1] Ad Stoffelen,[1] Anton Verhoef,[1] and Julia Figa-Saldaña[2]

Received 6 September 2010; revised 4 July 2011; accepted 1 August 2011; published 28 October 2011.

[1] High-resolution wind products based on space-borne scatterometer measurements by ASCAT and SeaWinds are used widely for various purposes. In this paper the quality of such products is assessed in terms of accuracy and resolution, using spectral analysis and triple collocation with buoy measurements and NWP model forecasts. An experimental ASCAT coastal product is shown to have a spectral behavior close to $k^{-5/3}$ for scales around 100 km, as expected from theory and airborne measurements. The NWP spectra fall off more rapidly than the scatterometer wind spectra starting at scales of about 1000 km. Triple collocation is performed for four collocated data sets, each with a different scatterometer wind product: ASCAT at 12.5 km and 25 km, and SeaWinds at 25 km processed in two different ways. The spectral difference between scatterometer wind and model forecast is integrated to obtain the representation error which originates from the fact that global weather models miss small-scale details observed by the scatterometers and the buoys. The estimated errors in buoy winds and model winds are consistent over the data sets for the meriodional wind component; for the zonal wind component consistency is less, but still acceptable. Generally, enhanced detail in the scatterometer winds, as indicated at high spatial frequencies by a spectral tail close to $k^{-5/3}$, results in better agreement with buoys and worse agreement with NWP predictions. The accuracy of the scatterometer winds is about 1 ms^{-1} or better. The calibration coefficients from triple collocation indicate that on average the ASCAT winds are slightly underestimated.

Citation: Vogelzang, J., A. Stoffelen, A. Verhoef, and J. Figa-Saldaña (2011), On the quality of high-resolution scatterometer winds, *J. Geophys. Res.*, *116*, C10033, doi:10.1029/2010JC006640.

1. Introduction

[2] Wind scatterometry is a widely used technique for measuring global ocean surface winds from space. Current operational applications include, among others, assimilation into global models for numerical weather prediction like that of the European Centre for Medium range Weather Forecasting (ECMWF) [*Hersbach and Janssen*, 2007] and detection of tropical and extratropical hurricanes for marine nowcasting [*Brennan et al.*, 2009].

[3] Scatterometers measure the radar cross section of the ocean surface. A Geophysical Model Function (GMF) provides the radar cross section as a function of the equivalent neutral wind vector at 10 m anemometer height, incidence angle, relative azimuth angle, radar frequency, and polarization [*Wentz and Smith*, 1999; *Hersbach et al.*, 2007]. Numerical inversion of the GMF yields the scatterometer wind measurement [*Stoffelen and Portabella*, 2006]. Due to the nature of radar backscatter from the ocean surface, this procedure usually provides more than one solution. These multiple solutions are referred to as ambiguities. If the scatterometer observations are to be assimilated in a numerical weather prediction (NWP) model, the ambiguities and their a-priori probabilities can be fed into the variational data assimilation scheme of that model and combined with other observations [*Stoffelen and Anderson*, 1997; *Portabella and Stoffelen*, 2004]. If, on the other hand, the scatterometer observations are intended as stand-alone information source for nowcasting, it is necessary to select the solution that is most likely the correct one. This is done in the ambiguity removal (AR) step.

[4] ASCAT is a scatterometer at C-band equipped with three arms, each with two radar antennas [*Figa-Saldaña et al.*, 2002]. It is carried by the MetOp-A satellite that was launched in 2006 and it is operated by the European Organisation for the Exploitation of Meteorological Satellites (EUMETSAT). It is planned that MetOp-A will be followed by MetOp-B in 2012 and MetOp-C in 2017, thus providing for at least 15 years of operational scatterometer data services. Level 1 processing is done by EUMETSAT; level 2 wind processing by the Royal Netherlands Meteorological Institute (KNMI) within the framework of the Ocean and Sea Ice Satellite Application Facility (OSI SAF). The level 2 processor, the ASCAT Wind Data Processor (AWDP) has been constructed within the SAF for Numerical Weather Prediction (NWP SAF). The SAF program is sponsored by EUMETSAT. The ASCAT 25-km (ASCAT-25)

[1]KNMI, De Bilt, Netherlands.
[2]EUMETSAT, Darmstadt, Germany.

0148-0227/11/2010JC006640

Table 1. Overview of the Scatterometer Wind Products Addressed in This Study

Name	Grid Size (km)	Issued by	Status
SeaWinds-NOAA	25	NOAA	discontinued
SeaWinds-KNMI	25	KNMI	discontinued
ASCAT-25	25	KNMI	operational
ASCAT-12.5	12.5	KNMI	operational
ASCAT-Box	12.5	KNMI	demonstration

and 12.5-km (ASCAT-12.5) products can be found on the OSI SAF web pages at KNMI (www.knmi.nl/scatterometer). The ASCAT coastal product is available experimentally. Its level 1 processing differs from that of the other ASCAT products in the way raw measurements are averaged to a triplet of radar cross sections per wind vector cell (WVC), see section 3 for more details.

[5] SeaWinds on board QuikSCAT is a rotating pencil-beam scatterometer operating at Ku-band [*Tsai et al.*, 2000]. This highly successful mission lasted from 1999 until November 2009. A near-real-time SeaWinds product (SeaWinds-NOAA) was issued by the National Oceanic and Atmospheric Administration (NOAA). Ambiguity removal was done with the Direction Interval Retrieval with Thresholded Nudging (DIRTH) algorithm [*Stiles et al.*, 2002]. The KNMI SeaWinds product (SeaWinds-KNMI) is derived from the SeaWinds-NOAA product using the SeaWinds Data Processor (SDP) that was developed within the NWP SAF. SDP features improved (rain) quality control [*Portabella and Stoffelen*, 2002a] and two-dimensional variational ambiguity removal (2DVAR) [*Vogelzang et al.*, 2009]. SeaWinds data are very noisy in the nadir part of its swath because its measurement geometry at nadir gives rise to broad minima in the GMF. *Vogelzang et al.* [2009] show that this noise is effectively suppressed in the SeaWinds-KNMI product by the Multiple Solution Scheme (MSS) in combination with 2DVAR. MSS retains the local wind vector probability density function after inversion rather than only a limited number of ambiguous solutions, which poorly represent the broad minima. This allows 2DVAR to select a wind vector that has slightly lower a-priori probability but much more spatial consistency, thus reducing noise.

[6] The aim of this paper is to characterize in detail the quality of operationally available scatterometer wind products in order to provide guidance to their users as to which product may be best suited for his or her application. Moreover, in the development of scatterometer wind products, processing options need to be traded off and a set of objective tools to do so must be developed. Two main issues generally appear in product comparisons. First, since not all products use the same quality control (QC) their geographical sampling may differ and thus over a given period different products may show different statistical characteristics. Second, the level of smoothing applied to suppress measurement noise may differ among products. Users may want to consider what amount of smoothing is appropriate for their application and thus may accept different levels of noise or spatial representation (smoothness).

[7] To address these two issues, we elaborated two tests for product comparison: (1) analysis of the wind component spectra to detect noise and assess the relative amount of small scale information, and (2) triple collocation with a representative set of ECMWF NWP data and buoy data to calculate error variances and calibration coefficients.

[8] The wind products considered here are listed in Table 1. The term "operational" must be taken in a broad sense, since this study addresses wind products that recently ceased (SeaWinds) as well as experimental products (ASCAT-Box). It also indicates that the data sets were produced to support operational forecasting in the first place, so the processing software may have been upgraded meanwhile. ASCAT was not corrected for equivalent neutral wind before January 2009, but since this correction is a constant of 0.2 ms^{-1} to the wind speed, it only affects the bias of the ASCAT winds, not their error standard deviation. Other upgrades of the processing software during the period of interest did not affect inversion, quality control, or ambiguity removal, so in this respect the scatterometer data set is homogeneous. The SeaWinds science product issued by the National Aeronautics and Space Administration (NASA) falls outside the scope of this study. However, *Portabella and Stoffelen* [2002b] find little statistical difference between collocated NASA and NOAA products.

[9] Spectra from aircraft measurements at various heights show an approximate k^{-3} behavior for scales larger than 1000 km and a $k^{-5/3}$ behavior for scales from about 500 km down to 3 km [*Nastrom et al.*, 1984; *Nastrom and Gage*, 1985]. *Freilich and Chelton* [1986] calculate spectra from wind measured with the Seasat-A Satellite Scatterometer (SASS) for scales up to 200 km, just on the edge of the $k^{-5/3}$ regime. *Chelton et al.* [2006] study spectra of QuikSCAT winds and find for scales below 1000 km a behavior that is slightly flatter than k^{-2}. *Patoux and Brown* [2001] calculate kinetic energy spectra over the Pacific from QuikSCAT measurements and find a k^{-2} behavior for scales between 1500 km to 50 km, with some flattening due to noise at the high frequency part of the spectrum. *Milliff* [2004] reports similar results for QuikSCAT zonal wind spectra over the Mediterranean, with an even more prominent noise floor.

[10] The triple collocation method was introduced by *Stoffelen* [1998]. Given a set of triplets of collocated measurements and assuming linear calibration, it is possible to simultaneously calculate the errors in the measurements and the relative calibration coefficients. The method has been applied to assess the accuracy of, e.g., ocean wave height [*Janssen et al.*, 2007] and ocean stress [*Portabella and Stoffelen*, 2009]. A complication in the triple collocation method is that the spatial resolution of global NWP models is much coarser than that of scatterometer or buoy measurements. This is handled by introducing the representation error, a correlated error between scatterometer and buoy measurements that represents small scale information missed by the NWP model, but captured by both scatterometer and buoy. *Stoffelen* [1998] estimated the representation error on basis of total variance and a $k^{-5/3}$ wind spectrum. Here the correlated error is calculated by integrating the difference between actual scatterometer and NWP spectra.

[11] The triple collocation method can give the measurement errors from the coarse resolution NWP model perspective or from the intermediate resolution scatterometer perspective, but not from the fine resolution buoy perspective without further assumptions on the local buoy measurement error. Signal present in buoy measurements but not in scatterometer measurements is therefore contained in the buoy

error. This perception of errors being scale dependent is very important in the concept of triple collocation. *Portabella and Stoffelen* [2009] apply the triple collocation method to individual buoys and find geophysical effects possibly caused by currents, sea state, and local wind climate. These effects are neglected here, but it can be expected that these effects add to the buoy errors. Since the main focus is on the quality of scatterometer winds, this is not considered as a serious drawback.

[12] In what follows the term resolution refers to the true spatial resolution of a measurement system (scatterometer, buoy, or NWP model), i.e., the size of the smallest details discernible. The resolution of scatterometer wind fields is hard to establish, because the gridded radar cross section multiplets from which wind vectors are calculated are obtained from different footprint shapes and different antenna orientations. Moreover, the ambiguity removal processing acts as a spatial filter. The resolution is not to be confused with the grid size on which scatterometer measurements or model data are presented.

[13] The relevant formulas for spectral analysis and triple collocation are summarized in section 2. The methods used for sampling and detrending are described in more detail, and an estimate for the precision in the triple collocation errors is given. Section 3 describes the data sets used. In this section the difference in level 1 processing between the ASCAT-Box product and the other ASCAT products is described. The results are presented in section 4. They were obtained for all winds speeds and for all ASCAT incidence angles and SeaWinds azimuth angles. It is shown that spectral analysis and triple collocation yield consistent results for the meridional wind component v. Consistency is less for the zonal wind component u but still acceptable when the SeaWinds-NOAA data set is left out of consideration. This product has a random error with a standard deviation of 1.2 ms^{-1} in u and 1.1 ms^{-1} in v, while the other products have smaller error standard deviations between 0.6 ms^{-1} and 0.8 ms^{-1} (errors averaged over all wind speeds and all incidence or azimuth angles). The calibration coefficients indicate that at high winds the KNMI products (ASCAT-12.5, ASCAT-25, and SeaWinds-KNMI) slightly underestimate the wind magnitude, while the SeaWinds-NOAA product overestimates it. Possible reasons for the deviant behavior of the SeaWinds-NOAA product are discussed in section 5. Here also the consequences for practical use are considered. The paper ends with the conclusions in section 6.

2. Analysis Methods

2.1. Spectral Analysis

[14] A scatterometer like SeaWinds or ASCAT measures the normalized radar cross section of the ocean surface. The cross sections are averaged on an approximately regular grid with size Δ, typically equal to 12.5 km or 25 km. The wind vector is then calculated from the gridded cross sections. In this study samples of the wind vector, in particular its zonal and meridional components u and v, are collected along the satellite track for each across-track Wind Vector Cell (WVC) separately. No samples in the across-track direction are collected. For each sample a spectrum is calculated, and all spectra are averaged, thus averaging over all possible across-track dependencies. The whole swath of ASCAT and SeaWinds is taken into consideration, including SeaWinds' outer and nadir parts of the swath.

[15] A prerequisite for spectral analysis with the Fast Fourier Technique (FFT) is that the samples do not contain missing values. In order to increase the number of valid samples, isolated missing WVCs, mainly due to QC, are filled by linear interpolation. Figure 1 shows the global density of accepted WVCs on a 1° × 1° grid for all SeaWinds-KNMI data at 25 km grid size from January 2009. The global density is defined as the number of WVCs in a 1° × 1° grid box that are member of a valid sample, divided by the total number of WVCs in all samples (so summing the global density over all grid boxes yields 1). Without interpolation (Figure 1, top) a total number of 9120 samples with length 128 is found, containing only 6.3% of all available data. Interpolation over isolated missing WVCs (Figure 1, bottom) increases the number of samples to 50740 containing 35% of all available data. Moreover, comparison of the two panels shows that interpolation decreases the highest density over the open ocean (blue and purple) and increases the relative contribution of coastal areas, thus leading to more representative sampling over the oceans. Interpolation over two or more missing WVCs only yields a few hundred additional valid samples. For ASCAT relatively few WVCs are QC-ed because rain has less impact on observations at C-band than at K_u-band and the effect of interpolation is less pronounced. Nevertheless, the same interpolation strategy will be followed for all scatterometer wind products.

[16] For a sampled wind component $z_i, i = 0,1,\ldots, N-1$ the one-sided wind spectral density ψ is defined as

$$\psi_j = \psi(k_j) = \begin{cases} \dfrac{\Delta}{N}|\hat{z}(k_j)|^2 & , \quad j = 0 \text{ or } j = \dfrac{N}{2} \\ \dfrac{\Delta}{N}\left[|\hat{z}(k_j)|^2 + |\hat{z}(k_{-j})|^2\right] & , \quad j = 1,\ldots,\dfrac{N}{2}-1 \end{cases} \tag{1}$$

with $\hat{z}$ the Fourier transform of z obtained using standard FFT techniques and k_j the spatial frequency given by

$$k_j = \frac{j}{N\Delta} \qquad j = -\frac{N}{2}+1,\ldots,\frac{N}{2} \tag{2}$$

[17] The mean square value of the wind component in the sample, $\langle z^2 \rangle$, is equal to the spectrum integrated over all values

$$\langle z^2 \rangle = \frac{1}{N\Delta}\sum_{j=0}^{N/2}\psi_j \tag{3}$$

[18] With this normalization, the variance in the interval (k_m, k_n) equals $\sum_{j=m}^{n}\Psi_j\Delta k$ with $\Delta k = (N\Delta)^{-1}$. The final spectrum is obtained by averaging the spectra from each individual sample.

[19] In this study a sample contains typically $N = 128$ points, covering a strip over the ocean of 3200 km (for wind products on a 25 km grid) or 1600 km (for wind products on a 12.5 km grid). This misses the largest-scale wind variations over the oceans caused by e.g., the trades as illustrated in Figure 2. This

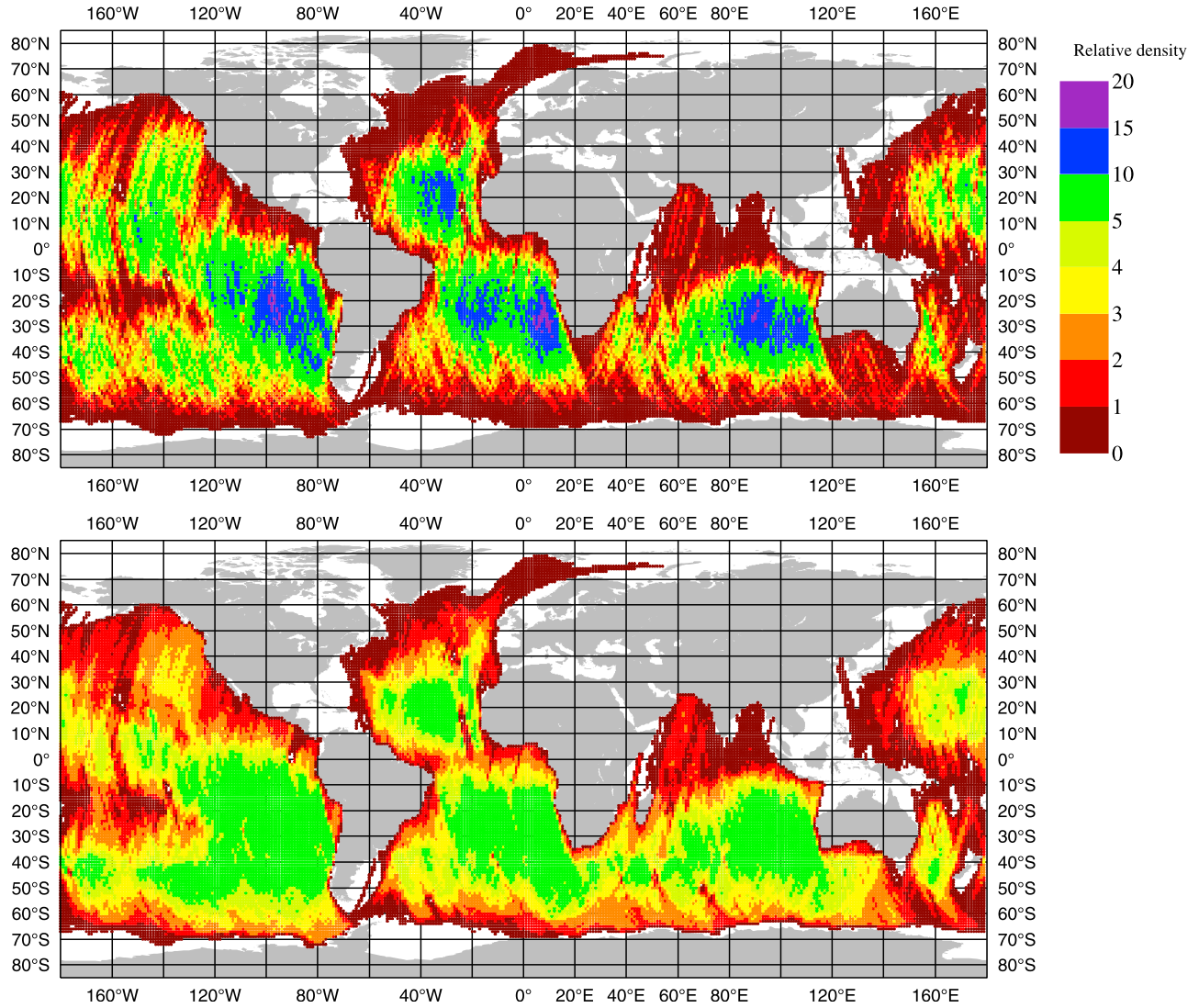

Figure 1. Global density of WVCs contributing to the wind spectrum for all SeaWinds-KNMI data from January 2009 (top) without interpolation and (bottom) with interpolation of isolated missing points.

figure shows the value of the zonal wind component u in the very first sample found in the January 2009 SeaWinds-KNMI data set (solid curve). There is a large difference between the value of u at the sample's start and end point due to large-scale variations. Since the FFT operation assumes a sample to be periodic, this difference acts as a sudden strong jump, adding a large contribution to the spectrum with shape k^{-2}. One could partially mitigate such unwanted effects by increasing the sample size, but then the number of valid samples decreases drastically as shown in Table 2.

[20] A way out is offered by detrending, i.e., removing the difference between the end values of the sample without affecting its information content at small scales. Several methods have been tried and three of them gave satisfactory results: (1) linear transformation (LT), $z_i' = a\, z_i + b$, with the coefficients a and b chosen such that the sample end points map to zero [*Errico*, 1985; *Frehlich and Sharman*, 2008]; (2) first differencing (FD), $z_i' = z_{i+1} - z_i$, which acts as a high pass filter that can be corrected for afterwards [*Percival and Walden*, 1993]; and (3) windowing, $z_i' = w_i z_i$, with w a common window function like the Hanning window [*Press et al.*, 1988] normalized as

$$\sum_{i=0}^{N-1} w_i^2 = N \tag{4}$$

[21] The average is subtracted from each sample, but this only affects the value of ψ_0. Figure 2 shows that these three methods effectively remove the difference between the first and last value in the sample. The spectral densities obtained with these methods have a maximum difference of 1% at most in the interval $[k_1, k_{N/2}]$ (no results shown). Since the spectra obtained with first differencing are corrected for the high pass filtering, they must conserve variance in the interval $[k_1, k_{N/2}]$. But this must also apply to the other methods, as they yield almost the same results. In the remainder of this paper the LT method is used because it gives results closest to first differencing. This has also been observed by D. B. Chelton (private communication, 2010). Note that the sample size for FD must be one larger than for the other methods. Another

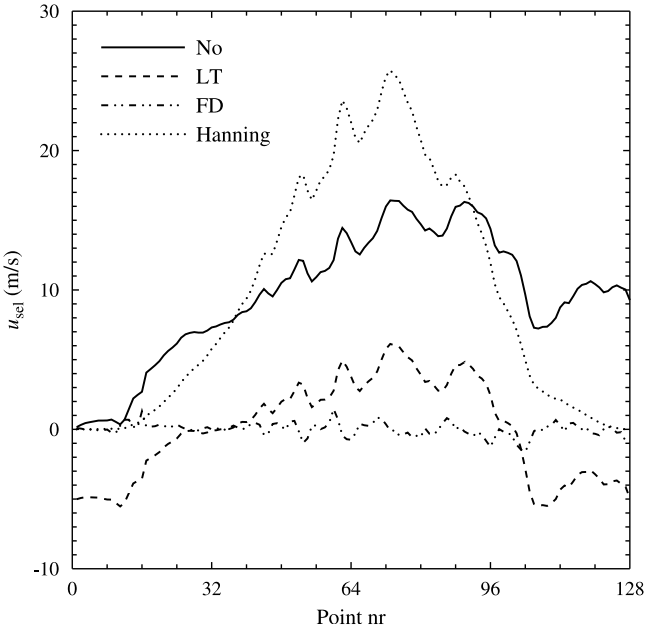

Figure 2. First sample of the zonal wind component u in the ASCAT-KNMI data of January 2009 data set. Shown are the raw sample values (solid curve) and the detrended sample values resulting from the linear transformation (LT, dashed curve), first differencing (FD, dot-dot-dashed curve), and Hanning windowing (dotted curve). The sample average has been removed for LT and FD.

detrending method that is closely related to windowing is application of a cosine taper [*Patoux and Brown*, 2001].

2.2. Triple Collocation

[22] Quantitative information on the precision of the scatterometer winds can be obtained from the triple collocation method introduced by *Stoffelen* [1998]. The key point in this method is that calibration and error calculation are combined in order to avoid the introduction of pseudo biases. The triple collocation method will be used here with collocated data from scatterometers, buoys, and NWP models.

[23] Supposing three measuring systems $X_i, i = 1,2,3$, measuring the same quantity t and assuming that for each system linear calibration suffices, the measurements satisfy

$$x_i = a_i t + b_i + \delta_i \tag{5}$$

where a_i and b_i stand for resp. the trend and bias calibration coefficients and δ_i for a random measurement error in system i. The random measurement errors are assumed free of bias, so $\langle \delta_i \rangle = 0$. Moreover, the variance of random measurement errors is assumed to be constant over the whole range of wind speeds, i.e., $\langle \delta_i^2 \rangle$ does not depend on t. This is an approximation, but *Stoffelen* [1998] has shown that (5) holds well for the wind components u and v in the range of wind speeds sampled by a scatterometer, but not for the wind speed or direction. From inspection of the scatterplots the authors conclude that this is also the case for the data used in this study (no results shown).

[24] Suppose now that system 1 stands for the buoys, system 2 for the scatterometer, and system 3 for the NWP background. Furthermore, choose the buoys as calibration reference, i.e., the system relative to which the two other systems are to be calibrated. Since the buoys and the scatterometer resolve smaller scales than the NWP background, the common signal t is defined on the NWP scale. As a consequence, the variance resolved by scatterometer and buoys but not by the NWP background will be represented in δ_i, i.e., as errors. Since scatterometer and buoys partially resolve the same scales, these errors will be correlated: $\langle \delta_1 \delta_2 \rangle = r^2$ where r^2 stands for the variance of the correlated part of the representativeness errors of buoys and scatterometer. The other error correlations are assumed to be zero. It should be stressed here that r^2 is not really an error but small-scale signal present in buoys and scatterometers but absent in the NWP background. Once r^2 is known, it can be corrected for to obtain the errors at the resolution of scatterometer and buoys, see below. Buoys reveal even finer details as scatterometers, but in the triple collocation method these details add to the buoy error, implying that the buoy wind error can't be verified at full resolution against NWP background or scatterometer winds.

[25] With these assumptions, all unknowns can be solved from all first and second order moments (including mixed moments) that can be formed from (5). The result for the error variances is

$$\varepsilon_1^2 = M_{11} - M_{12} + r^2 \quad , \quad \varepsilon_2^2 = M_{22} - M_{12} + r^2 \quad , \quad \varepsilon_3^2 = M_{33} - M_{31} \tag{6}$$

where $\varepsilon_i^2 = \langle \delta_i^2 \rangle$ is the desired error variance of system i from the perspective of the coarse resolution NWP model as indicated by the fact that the error variances of buoy and scatterometer are increased with the representation error. The error variances from the perspective of the finer resolution scatterometer measurements is obtained by subtracting r^2 from the buoy and scatterometer error variances ε_1^2 and ε_2^2, since it comprises a real signal, and adding it to the NWP background error variance ε_3^2, since this signal is not present in the NWP model. Further, $M_{ij} = \langle x_i x_j \rangle$, $i, j = 1,2,3$ stands for the second order (mixed) moment of data sets i and j. The result for the calibration trend coefficients of scatterometer and NWP model is, respectively

$$a_2 = \frac{M_{23}}{M_{31}} \quad , \quad a_3 = \frac{M_{23}}{M_{12} - r^2} \tag{7}$$

[26] The reader is referred to *Stoffelen* [1998] for a complete derivation of (6) and (7). Note the difference between the expression for a_3 above and the equivalent expression by *Stoffelen* [1998] which in our notation reads $a_3 = M_{23}/(M_{12} - a_2 r^2)$. This is because he started with $x_i = a_i(t + \delta_i)$

Table 2. Number of Valid Samples Found in the ASCAT-25 and SeaWinds-KNMI Data of January 2009 for Various Sample Lengths

	Number of Samples	
Sample Size	ASCAT-25	SeaWinds-KNMI
128	75863	50740
256	23255	6579
512	2534	12
1024	0	0

instead of (1), and estimated $r^2 = 0.75\ \mathrm{m^2 s^{-2}}$ for the scatterometer carried by the European Remote Sensing satellite (ERS-1) on the basis of the total variance and a $k^{-5/3}$ scatterometer wind spectrum. Therefore Stoffelen's representation error scales with a_2, and this scaling is explicitly shown in his paper. In this work r^2 will be calculated from observed scatterometer and NWP wind spectra, so it scales with both a_2 and a_3, see next subsection. This scaling is assumed implicitly in (6).

[27] It will be shown in section 4 that for low spatial frequencies (large spatial scales) the scatterometer and NWP wind spectra lie very close to each other, while for high spatial frequencies (small scales) the NWP spectrum drops dramatically compared to the scatterometer spectrum. This is due to numerical cut-off at small scales that beneficially suppresses undetermined small-scale structures in the ECMWF NWP model and thus prevents their detrimental upscale growth, which would deteriorate medium-range forecast skill. Assuming that the scatterometer spectrum represents the truth, the representation error can be estimated by integrating the difference between scatterometer spectrum ψ_{scat} and NWP spectrum ψ_{NWP} as

$$r^2 = \int_{k_{NWP}}^{k_{scat}} dk\ [\psi_{scat}(k) - \psi_{NWP}(k)] \tag{8}$$

[28] The upper integration limit of (8) is the highest spatial frequency observed by the scatterometer, $k_{scat} = (2\Delta)^{-1}$. The spatial scale associated with k_{scat} equals 2Δ, which is generally close to the actual spatial resolution of the scatterometer winds. The lower integration limit in (8) corresponds to the spatial frequency k_{NWP} at which the numerical cutoff in the NWP model starts to suppress small scales. The spatial scale associated with k_{NWP} is

$$s_{NWP} = \frac{1}{k_{NWP}} \tag{9}$$

[29] One expects s_{NWP} to be determined only by the characteristics of the NWP model used, but for the moment it will be considered as a free parameter. It will be shown in section 4 that it is of the order of 800 km for the ECMWF model. This is much larger than the model grid size due to numerical cut-off at small scale as mentioned before. It will also be shown in section 4 that in some cases the increment in r^2 with s_{NWP} may be so strong that for large s_{NWP} the triple collocation equation (6) produce negative results for the error variances. In such cases the method presented here cannot be applied.

2.3. Iteration

[30] The triple collocation method not only solves for the error variances of buoy, scatterometer, and background wind components, but also for the scaling of scatterometer and background wind components with respect to the buoy measurements. This affects the scatterometer and background wind spectra and, by (8), the representation error which now reads

$$r^2 = \int_{k_{NWP}}^{k_{scat}} dk\ \left[a_2^2\psi_{scat}(k) - a_3^2\psi_{NWP}(k)\right] \tag{10}$$

since the spectral density is proportional to the square of the wind component. This new value of the representation error will affect the triple collocation results, etc. Obviously, the problem must be solved iteratively starting with the uncalibrated spectra and $a_2 = a_3 = 1$. Since the scaling parameters a_2 and a_3 differ little from 1 in the cases considered here, as will be shown in section 4, iteration of (6), (7), and (10) converges in three or four steps. The convergence criterion is that the values of $\varepsilon_i^2, i = 1,2,3$, a_2 and a_3 remain constant within five decimal places. The results in section 4 were obtained after 10 iterations.

[31] If the scatterometer winds contain a white noise contribution, as is the case for the SeaWinds product issued by NOAA, the spectrum will tend to become constant at high spatial frequencies. This scatterometer white noise is not correlated with the buoy winds and thus should not contribute to the representation error. The white noise variance is calculated from the autocorrelation [*Vogelzang et al.*, 2009] and the corresponding spectral level is determined and subtracted from the scatterometer spectrum before computation of equation (10).

2.4. Accuracy of the Error Variances

[32] Finally the (statistical) accuracy of the error variances is considered. Little is known about the shape of the error distribution, but *Stoffelen* [1998] has shown that a Gaussian shape is a reasonable assumption for the wind components u and v. Neglecting the error in r^2, the error variance in the estimate of ε_i^2 equals

$$\mathrm{Var}\left(\varepsilon_i^2\right) = \frac{2\varepsilon_i^4 + \varepsilon_i^2\varepsilon_j^2}{N_{TC}} \tag{11}$$

where N_{TC} stands for the number of collocated triplets, $j = \mathrm{mod}(i,3) + 1$, and $i = 1,2,3$. Equation (11) gives an indication of how precise the error variance estimates are.

3. Data

[33] This study uses SeaWinds (on board QuikSCAT) and ASCAT scatterometer data, ECMWF model forecasts, and buoy measurements. The data set for spectral analysis consists of all data from SeaWinds and ASCAT recorded in January 2009. The SeaWinds-NOAA product is obtained from NOAA. It is already collocated with forecasts from the model of the National Center for Environmental Prediction (NCEP). The SeaWinds-NOAA product is reprocessed at KNMI with SDP using among others improved quality control [*Portabella and Stoffelen*, 2002a] and 2DVAR in combination with MSS in order to minimize the observation noise in the SeaWinds-wind product caused by broad minima in the GMF, particularly for nadir view [*Vogelzang et al.*, 2009]. The SeaWinds-KNMI product uses ECMWF short-range forecasts as background.

[34] The level 1 ASCAT radar cross section data are obtained from EUMETSAT and processed to operational level-2 wind products at KNMI using AWDP. Ambiguity removal is done with 2DVAR, but MSS is not needed here because ASCAT's measurement geometry leads to narrow wind minima throughout the swath [*Stoffelen and Portabella*, 2006].

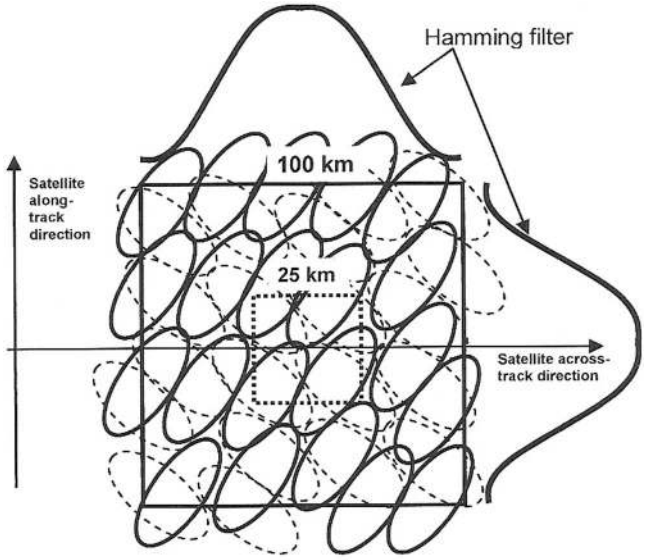

Figure 3. Radar cross section averaging in level 1 processing (schematic).

[35] In order to reduce the measurement noise and following the same approach used for the ERS Scatterometer level-1 processing, the ASCAT level-1 cross-section data are calculated by averaging individual backscatter measurements. The weighting function chosen for this averaging is a two-dimensional Hamming window, designed to provide noise reduction and spatial resolution [*Figa-Saldaña et al.*, 2002], allowing at the same time the possibility of oversampling the data without introducing spatial aliasing effects. Measurement noise, which occurs on WVC level, would cause spectra to saturate to a constant level at high frequencies. Spatial aliasing, on the other hand, mirrors undersampled high frequencies (i.e., higher than $k_{scat} = (2\Delta)^{-1}$) to frequencies below k_{scat}. Since wind spectra fall off at least as $k^{-5/3}$, spatial aliasing is expected to lead at most to a very modest elevation of the spectral tail.

[36] The individual backscatter samples prior to the averaging are centered in a square area with sides four times as large as the grid size of the wind product. This is sketched in Figure 3 for the ASCAT-25 product. For the ASCAT-12.5 product all dimensions have to be divided by 2. The black square with sides of 100 km is the cell in which the radar cross-section is calculated for each beam by averaging all individual measurements indicated as solid ellipses for the fore beam and as dashed ellipses for the aft beam. The mid beam is not shown for reasons of clarity of the figure. As a result of the choice of spatial averaging window, most of the contribution originates from the central 50 km × 50 km, though the average also contains some contribution further away. This prevents wind estimations closer to the coast than about 70 km because of the large land reflectivity.

[37] One would expect that box averaging, e.g., averaging only individual measurements that have their center within the dotted box in Figure 3, would result in more small scale detail, but possibly at the expense of some noise or aliasing. Noise may be easily suppressed by increasing the box size. Concerning spatial aliasing, one should realize that the radar cross section, σ^0, within the dotted box is not sampled by a point response function, but multiple times with a field of view of approximately 3 km (along fan beam) by 25 km (across fan beam). So, when considering all FOVs with centers within a given WVC, the integrated FOV (IFOV) for that WVC will be an area function extending up to 25 km outside the WVC in the direction across the fan beam. It is expected that this σ^0 contribution outside the WVC acts to suppress spatial aliasing effects, since neighboring WVCs have overlapping IFOVs for each beam. Again, increasing the box size at fixed sampling Δ, would also reduce spatial sampling artifacts (aliasing), if present.

[38] Since ASCAT has the three fan beams pointing in directions differing by 45° in azimuth, the "egg" shape of the IFOV will extend in different directions as well. Hence, the three beams in any WVC do not sense exactly the same area and therefore the three σ^0s do not agree with one unique wind, but rather with slightly different winds, as sampled by the different IFOVs. This causes some noise in the wind inversion, named geophysical noise [*Portabella and Stoffelen*, 2006]. Geophysical noise is generally well explained by the expected wind variability on the ocean surface, the sensitivity of the geophysical model function, and the difference in IFOV of the different beams in a WVC. Moreover, it is found to be substantial only below 5 m/s and it is not expected to generate much spurious noise in the retrieved winds [*Portabella and Stoffelen*, 2006].

[39] As a preparation for the ASCAT coastal product, EUMETSAT produced a level 1 test set in which the radar cross-sections were obtained by box averaging over the central 19.5 km × 19.5 km on a 12.5 km grid. This product, further referred to as ASCAT-Box, is available for the period December 16, 2008 to January 11, 2009. In this study only the data of January 2009 will be used.

[40] The triple collocation method not only requires collocation of scatterometer data with NWP forecasts, but also with high-quality buoy measurements. These are sparse over the ocean, so the triple collocation requires data from a much larger time span. Buoy collocation statistics are moreover seasonally dependent, such that a full year needs to be acquired in order to obtain globally representative statistics. Table 3 shows the collocation period for the various scatterometer products. The buoy measurements are obtained from ECMWF's Meteorological Archival and Retrieval System (MARS) at www.ecmwf.int/services/archive. Only data from buoys not blacklisted by ECMWF are used. Buoys are blacklisted by ECMWF when they show large differences with the model fields [*Bidlot et al.*, 2002]. Most of the accepted buoy data is from the Tropical Atmosphere Ocean (TAO) buoys and from buoys off the coasts of the U.S.A. and Europe, see Figure 4.

Table 3. Triple Collocation Data Acquisition Periods Used in This Study

Product	Start Date	End Date
SeaWinds-NOAA	Nov 1, 2007	Nov 30, 2009
SeaWinds-KNMI	Nov 1, 2007	Nov 30, 2009
ASCAT-25	Nov 1, 2007	Nov 30, 2009
ASCAT-12.5	Oct 1, 2008	Nov 30, 2009

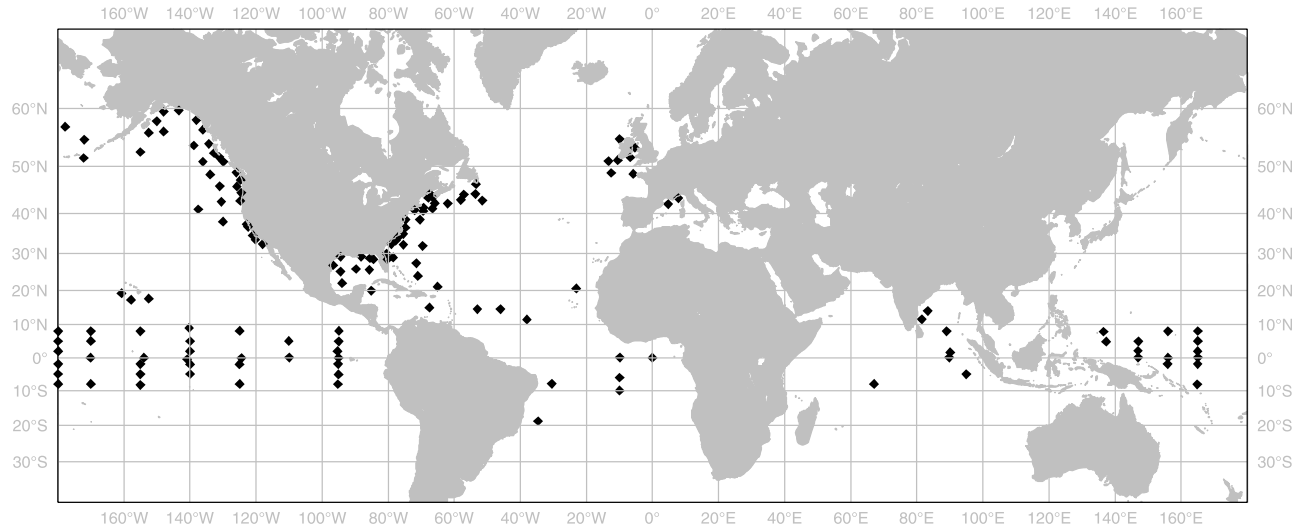

Figure 4. Location of buoys used in triple collocation.

[41] Since the ASCAT-Box product is available only for a limited period of time, it is not included in the triple collocation exercise.

4. Results

4.1. Spectra

[42] Figure 5 (left) shows the spectra of the wind component u and Figure 5 (right) shows the spectra of the wind component v for the various operational wind products considered here. The spectra are averaged over all WVC numbers across the swath. No calibration resulting from triple collocation has been applied to the spectra—this would shift the spectra slightly upward or downward. The spectra in Figure 5 agree with those obtained by other authors [e.g., *Chelton et al.*, 2006].

[43] The red curves show the ECMWF background spectra for the same samples as the ASCAT-25 data (solid red) and the SeaWinds-KNMI data (dotted red). Though the sampling is different, the resulting spectra are very similar. The green curves show the spectra for ASCAT-25 (solid green), ASCAT-12.5 (dashed green), and ASCAT-Box (dotted green); the blue curves spectra of SeaWinds-KNMI (solid) and SeaWinds-NOAA (dashed). The black dotted curve shows a $k^{-5/3}$ spectrum at arbitrary level. According to the aircraft measurements of *Nastrom and Gage* [1985] and the turbulence theory of Kolmogorov the wind spectra should follow this behavior for scales smaller than about 500 km (spatial frequency $2\ 10^{-6}$ m^{-1}). Most of the spectra in Figure 5 fall off faster, except for a noise contribution at the smallest scales in the scatterometer spectra. Only the ASCAT-12.5 spectrum of the meridional wind component and both ASCAT-Box spectra show a behavior close to $k^{-5/3}$. This is a very encouraging result for further developing the ASCAT coastal product. The ASCAT-12.5 and ASCAT-Box spectra show a bump for k between 10^{-5} m^{-1} and 10^{-4} m^{-1} which is also observed in spectra from high resolution NWP output [*Frehlich and Sharman*, 2008]. Note that the ASCAT-Box spectra show no clear sign of noise (flattening of tail) nor spatial aliasing (tail elevation), so replacing the standard Hamming averaging with box averaging does not adversely affect the quality of the radar cross section triplets.

[44] One might conclude from Figure 5 that the SeaWinds-NOAA product contains more small-scale information than the SeaWinds-KNMI product. However, the SeaWinds-NOAA product, obtained with DIRTH as ambiguity removal method, is known to contain a considerable amount of observational white noise, notably at nadir. *Vogelzang et al.* [2009] show that this noise is removed when processing the data with MSS in combination with 2DVAR. These authors also provide a method to estimate the white noise variance from the size of the discontinuity of the autocorrelation (or covariance) at lag size zero. The autocorrelations were calculated for each sample that was used for the spectra and averaged, yielding estimated white noise variances of 0.23 m^{2}s^{-2} in u and 0.13 m^{2}s^{-2} in v for SeaWinds-NOAA and zero variance for the other data sets. Note that in the scale of Figure 5, with a spatial frequency range of $2\ 10^{-5}$ m^{-1}, a noise variance of 0.2 m^{2}s^{-2} corresponds to a spectral level of 10^{-4} m^{2}s^{-2}. The noise in the SeaWinds-NOAA spectra shows up as a constant contribution near the tail, somewhat above the level expected from the white noise variance estimate. Also the other scatterometer spectra show some flattening, but not as pronounced.

[45] The SeaWinds-KNMI spectra are somewhat closer to the ECMWF model spectra than the ASCAT-25 spectra, except for v at the highest spatial frequencies. Apparently, 2DVAR after MSS reduces noise at the cost of some information loss at intermediate scales due to the smooth fitting functions used. However, since the spectra are made at different locations on the globe, sampling may also contribute.

4.2. Representation Error

[46] Figure 6 shows the representation error variance r^2 as a function of s_{NWP} after iteration of (6), (7), and (10) has converged. The values for r^2 are largest for the zonal component of SeaWinds-NOAA and smallest for the zonal component of SeaWinds-KNMI, as expected from the spectra in Figure 5. The value of 0.75 m^{2}s^{-2} used by *Stoffelen* [1998] for ERS data is reached by ASCAT-12.5 for s_{NWP} around 500 km at

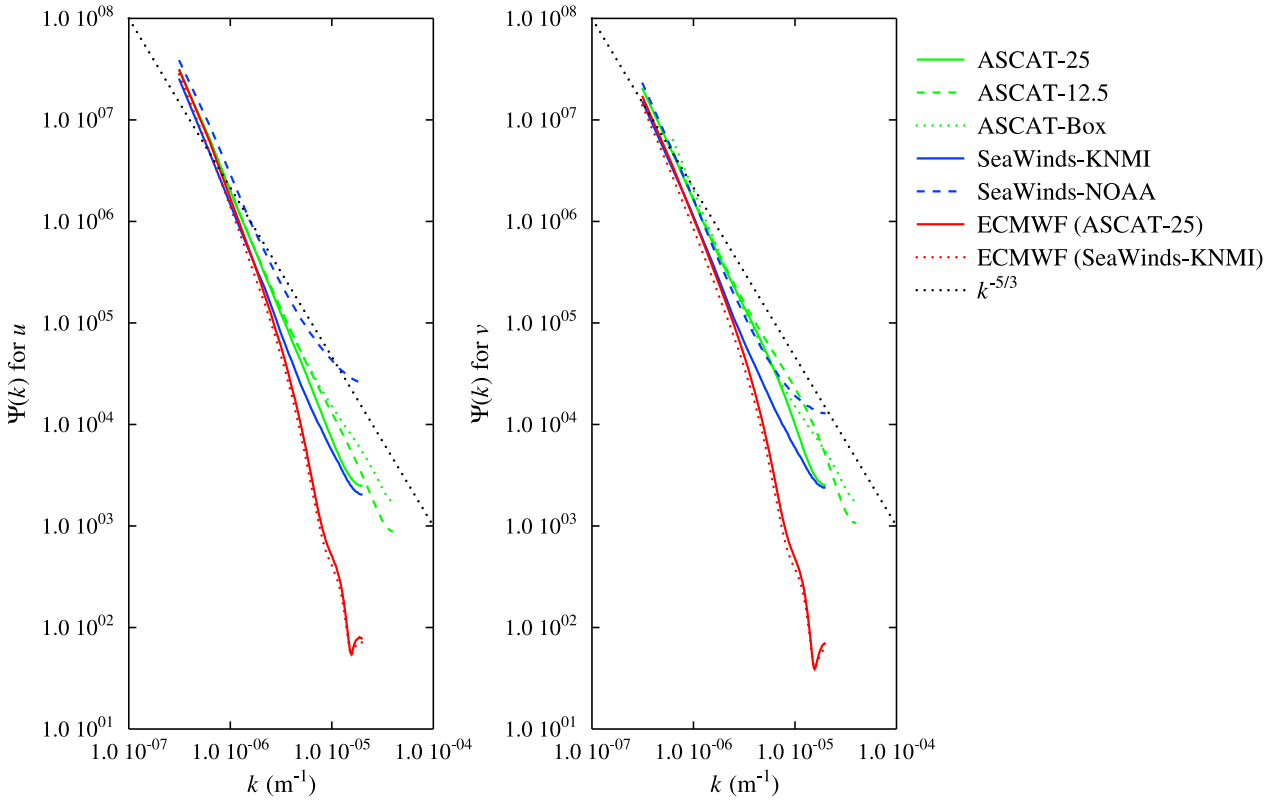

Figure 5. Spectra of the ASCAT-25 (solid green), ASCAT-12.5 (dashed green), ASCAT-Box (dotted green), SeaWinds-KNMI (solid blue), and SeaWinds-NOAA (dashed blue) wind products for (left) the zonal wind component u and (right) the meridional wind component v. The spectrum for the ECMWF background wind is given in red for the same sampling as ASCAT-25 (solid) and SeaWinds-KNMI (dotted).

u and 1200 km at v. For ASCAT-25 these values are higher: around 1200 km for u and beyond 1600 km for v. The representation error for SeaWinds-KNMI is smaller than 0.75 m^2s^{-2} over the whole range of s_{NWP}, most likely due to the fact that removal of observation noise leads to smoothing at intermediate scales.

4.3. Triple Collocation

[47] Figure 7 shows the triple collocation error estimates for the four collocation data sets as a function of s_{NWP}. Figure 7 (left) pertains to u, the right hand one to v. The curves for ε_{buoy}, ε_{scat}, and ε_{back} are in blue, red, and green, respectively. Solid curves indicate collocation results for ASCAT-12.5, dashed curves for ASCAT-25, dash-dotted curves for SeaWinds-KNMI and dotted curves for SeaWinds-NOAA. The representation errors were calculated on the spatial frequency grid and then linearly interpolated to a regular spatial 50 km grid.

[48] Ideally, one would expect that the three blue curves in each panel cross at one point, since the buoy errors should be independent of the scatterometer wind product. The same argument holds for the green curves representing the error in the ECMWF background. This holds well for v: the buoy errors are within 0.037 m^2s^{-2} for s_{NWP} = 700 km while the ECMWF errors are within 0.035 m^2s^{-2} for s_{NWP} = 1100 km. This is precisely in the range where the ECMWF spectra in Figure 5 start to deviate from the scatterometer spectra.

[49] The situation for u is less clear, because the representation error for the SeaWinds-NOAA data set is overestimated,

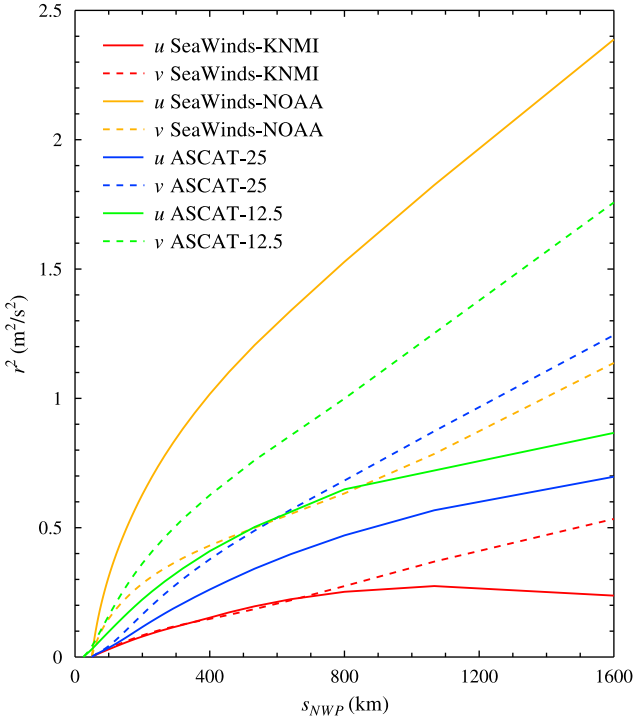

Figure 6. Representation error variance of u (solid curves) and v (dashed curves) as a function of s_{NWP}. The color of the curve indicates the type of wind product.

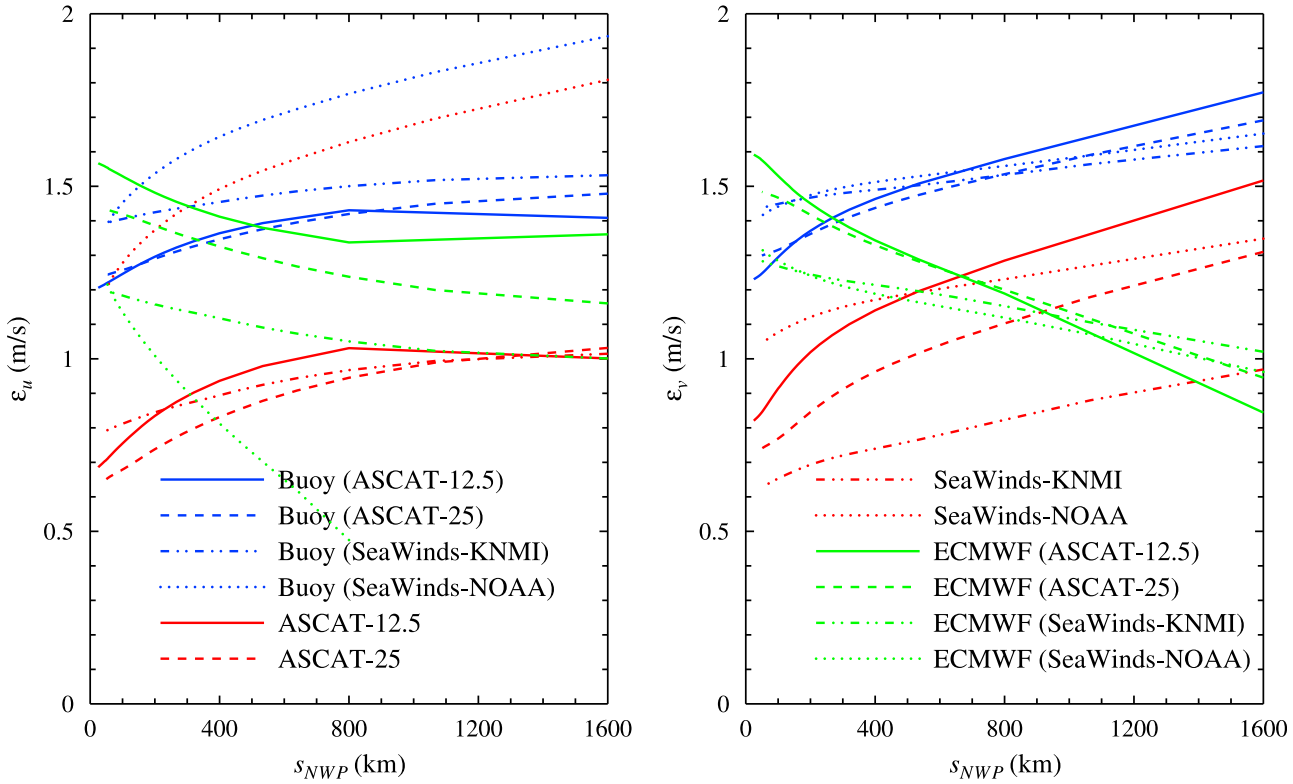

Figure 7. Error standard deviations obtained with triple collocation as a function of s_{NWP} for (left) u and (right) v. The blue curves are for the buoys, the red curve for the scatterometer wind products, and the green curves for the ECMWF background. Collocation results for ASCAT-12.5 are given by solid curves, those for ASCAT-25 by dashed curves, and those for SeaWinds-KNMI by dotted curves.

causing the triple collocation method to find negative variances for s_{NWP} larger than 900 km. If SeaWinds-NOAA is excluded, the other data sets have a minimum spread of 0.072 m^2s^{-2} at s_{NWP} = 950 km in the buoy errors and 0.28 m^2s^{-2} at s_{NWP} = 800 km in the ECMWF errors.

[50] Excluding the SeaWinds-NOAA data set, the sum of the spreads in buoy and ECMWF error standard deviations has a minimal value of 0.36 ms^{-1} in u at s_{NWP} = 800 km and of 0.092 ms^{-1} in v at s_{NWP} = 850 km. The corresponding error standard deviations and representation errors are listed in Table 4. An indication of the precision in each of the error standard deviations, σ, can be obtained from (11) and lies between 0.01 and 0.02 ms^{-1}, depending on the value of the standard deviation itself and the number of points in the collocation data set. Table 4 shows that for v both the buoy and the ECMWF errors are well within the 3σ range, even when the SeaWinds−NOAA data set is taken into consideration. For u the spread in the error standard deviations is larger, notably for the ECMWF model, where the spread is almost 0.3 ms^{-1}. One can interpret this as the ECMWF error lying between 1.0 and 1.3 ms^{-1}, which is still useful as an error estimate.

[51] The results in Table 4 are with respect to the resolution of the ECMWF model, so the common small-scale variance of buoy and scatterometer winds have been considered as a correlated error. To arrive at the errors with respect to the scatterometer resolution, the representation error variance must be subtracted from the scatterometer and buoy error variances and added to the ECMWF error variance. These results are shown in Table 5. Note that the resolved scales of the different products are not identical; they become smaller going from SeaWinds-KNMI via ASCAT-25 to ASCAT-12.5, following the size of the representation error. SeaWinds-NOAA does not follow this trend.

[52] Table 5 shows that the ASCAT-12.5 product lies closer to the buoys and further from the ECMWF model than the

Table 4. Triple Collocation Error Standard Deviations and Representation Error Variances With Respect to the Scales Resolved by the ECMWF Model

Data Set	Buoy		ECMWF		Scatterometer				
	ε_u (ms^{-1})	ε_v (ms^{-1})	ε_u (ms^{-1})	ε_v (ms^{-1})	ε_u (ms^{-1})	ε_v (ms^{-1})	r_u^2 (m^2s^{-2})	r_v^2 (m^2s^{-2})	Number of Points
ASCAT-12.5	1.44	1.59	1.32	1.18	1.05	1.29	0.63	1.00	32317
ASCAT-25	1.43	1.54	1.23	1.19	0.96	1.11	0.49	0.69	54187
SeaWinds-KNMI	1.51	1.54	1.04	1.14	0.98	0.84	0.33	0.31	76947
SeaWinds-NOAA	1.79	1.56	0.39	1.12	1.65	1.24	1.28	0.44	95195

Table 5. Triple Collocation Error Standard Deviations With Respect to the (Different) Scales Resolved by the Different Scatterometer Wind Products

	Buoy		ECMWF		Scatterometer	
Data Set	ε_u (ms^{-1})	ε_v (ms^{-1})	ε_u (ms^{-1})	ε_v (ms^{-1})	ε_u (ms^{-1})	ε_v (ms^{-1})
ASCAT-12.5	1.21	1.23	1.54	1.55	0.69	0.82
ASCAT-25	1.24	1.30	1.42	1.45	0.65	0.74
SeaWinds-KNMI	1.40	1.44	1.19	1.27	0.79	0.63
SeaWinds-NOAA	1.39	1.41	1.20	1.30	1.20	1.04

ASCAT-25 product, in agreement with the earlier observation that ASCAT-12.5 contains more small scale information. The ASCAT-12.5 product has an error slightly larger than the ASCAT-25 product, though the differences are of the same order as the precision estimates from (11). Moreover, the ASCAT-12.5 product has $1.24^2 - 1.21^2 = 0.07$ m^2s^{-2} more variance in u with respect to the buoy than the ASCAT-25 product, while its error variance is only $0.69^2 - 0.65^2 = 0.05$ m^2s^{-2} higher. For v the increase in variance is $1.30^2 - 1.23^2 = 0.18$ m^2s^{-2} while the increase in error is $0.82^2 - 0.74^2 = 0.12$ m^2s^{-2}. This shows that compared to the ASCAT-25 product, the small scale signal added in the ASCAT-12.5 km product is larger than the error increase.

[53] The SeaWinds-KNMI product lies closest to the ECMWF model and differs more from the buoys than the ASCAT products. This is due to 2DVAR in combination with MSS which reduces noise in the SeaWinds data at the cost of some loss in small details. The SeaWinds-KNMI data are more precise in v than in u; for ASCAT the situation is opposite. The SeaWinds-NOAA data set yields reasonable values for the errors at scatterometer resolution: the errors for buoy and ECMWF model are similar as those obtained with SeaWinds-KNMI, while the error in the scatterometer wind itself is much larger. However, due to the different behavior of SeaWinds-NOAA in Figure 7 and Table 4 this result must be taken with care.

[54] The triple collocation method also gives the calibration coefficients with respect to the buoys. These are listed in Table 6 for the scatterometers and the ECMWF background. Ideally, the ECMWF calibration should be the same for each data set. Table 6 shows that this is indeed the case for the meridional component of the ECMWF wind, while for the zonal wind component the differences are larger, with SeaWinds-NOAA again as clear outlier as far as the scaling coefficients a are considered. The bias corrections in Table 6, used to make the average wind components equal to zero, are small. Neglecting them does not significantly alter the triple collocation results (no results shown).

[55] The linearly calibrated scatterometer wind components $\widetilde{u}_{scat}$ and $\widetilde{v}_{scat}$ satisfy

$$\widetilde{u}_{\mathrm{scat}} = a_u u_{\mathrm{scat}} + b_u \quad , \quad \widetilde{v}_{\mathrm{scat}} = a_v v_{\mathrm{scat}} + b_v \tag{12}$$

[56] Table 6 shows that the calibration biases are small: $b_u \approx 0.2$ ms^{-1} and b_v is negligible. This implies that at high wind speeds, where both biases may be neglected, the scatterometer wind is underestimated when $a > 1$ and overestimated when $a < 1$. Table 6 shows that at high winds the ASCAT and SeaWinds-KNMI products underestimate the true wind speed, while SeaWinds-NOAA overestimates it. This holds, of course, averaged over all scatterometer nodes and geographical zones as well as within the assumptions made in the triple collocation method. This may help to explain why *Sienkiewicz et al.* [2010] observe fewer cyclones with hurricane force with ASCAT than previously with SeaWinds.

[57] Application of the scaling coefficients to the spectra in Figure 5 shifts spectra upward when $a > 1$ and downward when $a < 1$, thus decreasing the differences in spectral level at small spatial frequencies. Figure 8 shows the calibrated spectra. Compared to Figure 5 the difference between the various spectra at small spatial frequency (large spatial scales) has become smaller, though it has not disappeared.

[58] Since the spectra were obtained from different data sets than the triple collocation results, seasonal and/or regional effects might play a role. To check this, each data set was split in two subsets, one with latitude between −15° N and +15° N and the other with latitude between +25° N and + 55° N. Spectral calculation and triple collocation were repeated for the subsets, resulting in some very small changes in the error standard deviations for SeaWinds-NOAA and no significant effects at all for the other data sets (no results shown). This indicates that seasonal and regional effects are small for the data sets considered here.

5. Discussion

5.1. SeaWinds-NOAA Data Set

[59] The different behavior of the SeaWinds-NOAA data set cannot be explained by underestimation of its white noise content: good agreement with the other data sets is obtained only when the noise level is increased by an order of magnitude (no results shown), but that is not realistic in view of the spectra in Figures 5 and 8. Restriction of the SeaWinds-NOAA triple collocation data to those data points shared with the SeaWinds-KNMI set in order to mimic the more restrictive KNMI quality control only leads to marginal improvement.

[60] A possible explanation is indicated by the spectra in Figures 5 and 8. If the spectral shape of ASCAT-Box is

Table 6. Triple Collocation Results for the Calibration Coefficients of the Scatterometer Winds and the ECMWF Background Relative to the Buoy Measurements

	Scatterometer				ECMWF			
Data Set	a_u	b_u (ms^{-1})	a_v	b_v (ms^{-1})	a_u	b_u (ms^{-1})	a_v	b_v (ms^{-1})
ASCAT-12.5	1.012	0.19	1.008	−0.01	1.032	0.32	1.043	0.09
ASCAT-25	1.021	0.18	1.009	0.01	1.020	0.29	1.039	0.10
SeaWinds-KNMI	1.048	0.28	1.030	0.01	1.011	0.35	1.039	0.07
SeaWinds-NOAA	0.980	0.13	0.969	−0.02	0.981	0.35	1.039	0.06

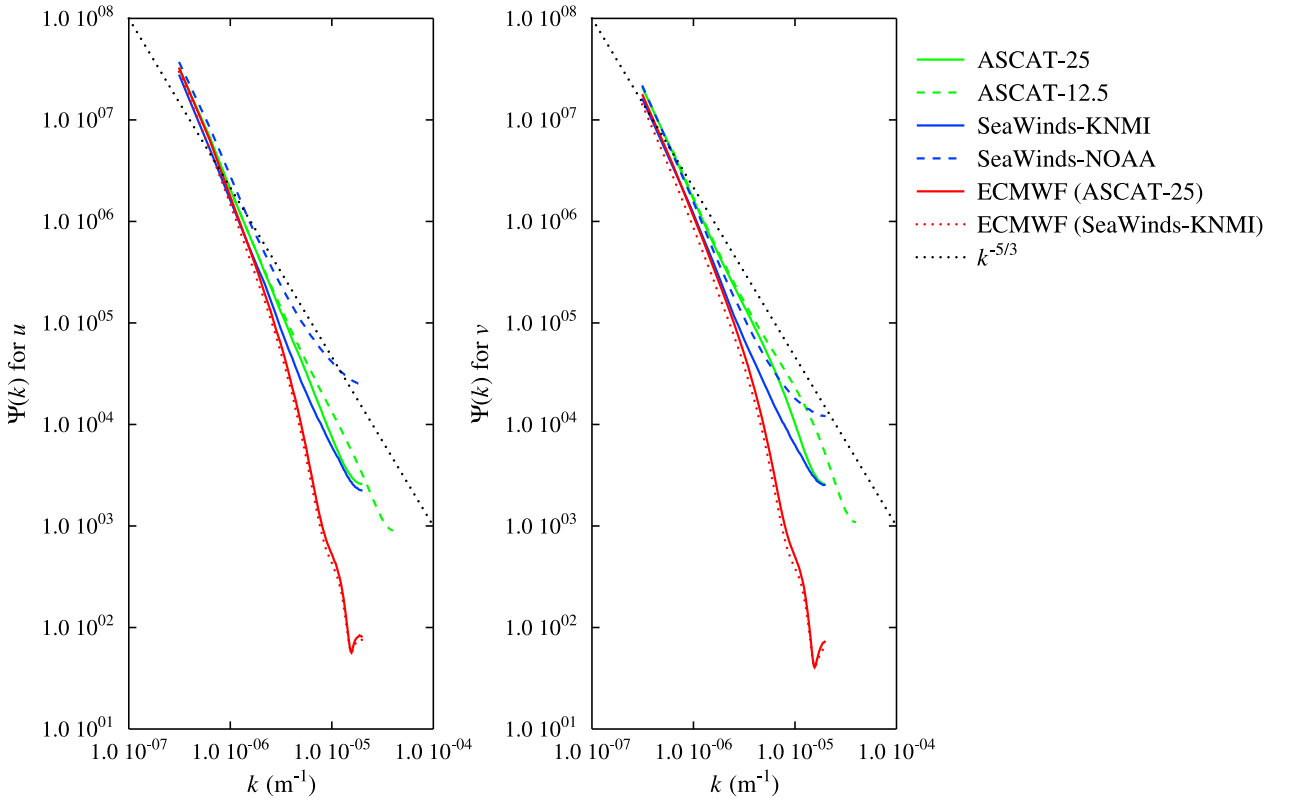

Figure 8. Calibrated wind spectra for (left) *u* and (right) *v*.

considered to be the most truthful, it would provide an estimate of the maximum representation error. Any spectral variance in excess of ASCAT-Box is likely to be error that will not correlate with buoy wind data. Therefore it should not contribute to the representation error. If the excess variance is caused by white noise of known strength, the spectrum is corrected for it, but if it is caused by spatially correlated noise (red noise) no compensation is possible unless the spectral characteristics are known. As a consequence, the representation error is overestimated following the procedure followed here. Figure 5 shows that this holds in particular for the zonal wind component of SeaWinds-NOAA.

[61] Correlated noise in the SeaWinds-NOAA product may be introduced by the spatial filter contained in DIRTH. Since ASCAT has well-defined double minima all over the swath and 2DVAR as a very high success rate for ASCAT data, AWDP is not expected to generate spatially correlated errors. This view is supported by the scatter diagrams of scatterometer wind speed and direction versus buoy wind speed and direction shown in Figure 9. The wind speed diagram for SeaWinds-NOAA (Figure 9, top left) resembles that of SeaWinds-KNMI (Figure 9, bottom left), though the SeaWinds-NOAA wind speed distribution is a little broader. The wind direction scatter diagram for SeaWinds-NOAA (Figure 9, top right) shows some increase in directional retrievals outside the central band for SeaWinds wind directions around 90° and 270°, visible in Figure 9 as bands with more yellow and green colors and less red and orange. The corresponding directional scatter diagram for SeaWinds-KNMI (Figure 9, bottom right) does not show such bands. This indicates ambiguity removal errors in the SeaWinds-NOAA product that tend to produce more zonal winds. Such errors are generally spatially correlated and are most probably the cause of the different behavior of SeaWinds-NOAA.

5.2. Consequences for Practical Use

[62] The results in the previous section show that the SeaWinds-KNMI and ASCAT wind products have about the same quality, though SeaWinds-KNMI is smoother. SeaWinds-NOAA has larger error but is still more precise as ECMWF forecasts and buoy measurements (on the scale of the scatterometers). For ocean studies involving eddy scales the ASCAT wind products are to be preferred, since eddy scales are smoothened out in SeaWinds-based products.

[63] The fact that ASCAT tends to underestimate the wind while SeaWinds overestimates it may account for the fact that with ASCAT less cyclones of hurricane force are detected than previously with SeaWinds [*Sienkiewicz et al.*, 2010]. Improvements in the GMF can fix these problems.

[64] It must be stressed here that the findings of this paper were based on global statistics. In particular wind speed effects, regional and seasonal differences, as well as WVC dependencies caused by incidence angle (ASCAT) or observation geometry (SeaWinds) were averaged over. Also the variance of random measurement errors is taken constant over the whole range of wind speeds in the data set, and higher order calibration effects are neglected. Study of such effects with the methods outlined here requires larger data sets and will be the subject of future work.

6. Conclusions

[65] The SeaWinds-NOAA product is known to contain observation noise at nadir, manifesting itself in the spectrum

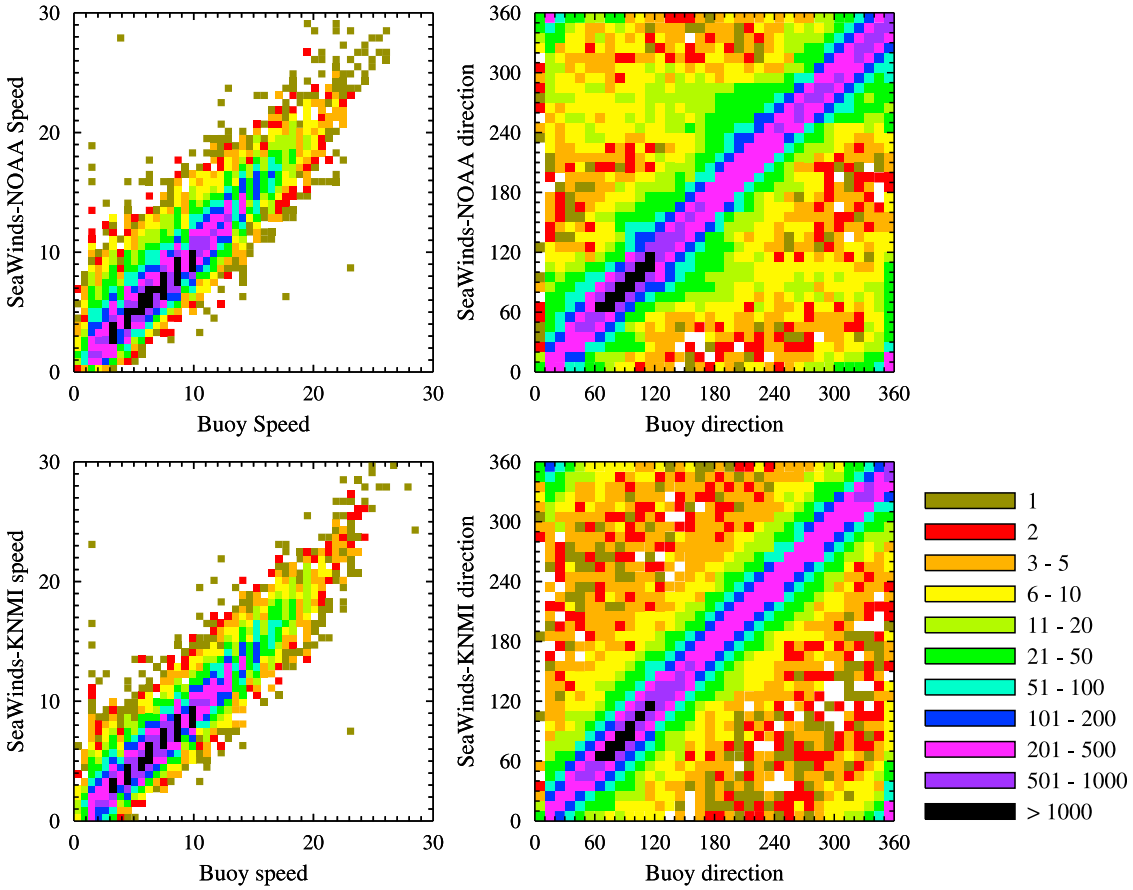

Figure 9. Scatter diagrams for (left) scatterometer wind speed versus buoy wind speed and (right) scatterometer wind direction versus buoy wind direction for (top) the SeaWinds-NOAA and (bottom) SeaWinds-KNMI triple collocation data sets.

as a noise floor at high frequencies. In the SeaWinds-KNMI product the noise is filtered out by application of 2DVAR in combination with MSS. However, the spectra show that this results in some loss of detail at intermediate and small scales. The ASCAT-25 wind product contains more intermediate scale information than the SeaWinds-KNMI product. The ASCAT-12.5 product reveals even more details, but most details are shown by the experimental ASCAT-Box product. Its spectrum behaves close to $k^{-5/3}$ for scales around 100 km.

[66] Triple collocation was done for a selected number of ocean buoys, ECMWF model predictions, and the ASCAT-12.5, ASCAT-25, SeaWinds-KNMI, and SeaWinds-NOAA scatterometer wind products. It was assumed that linear calibration suffices and that the distribution of random measurement errors is taken constant over the whole range of wind speeds encountered. Also regional and seasonal effects as well as WVC dependencies caused by incidence angle (ASCAT) or observation geometry variations (SeaWinds) were neglected, so the triple collocation results yield global averages of the calibration coefficients and error variances. The representation error was calculated by integrating the difference between the scatterometer and background spectra from the smallest scale to a variable scale s_{NWP}. The error standard deviations as a function of s_{NWP} shows minimum spreading at $s_{NWP} = 800$ km for u and at $s_{NWP} = 850$ km for v, as expected from the spectra. This excludes the SeaWinds-NOAA data set because its representation error becomes so large for $s_{NWP} > 900$ km that the triple collocation method produces negative variances at u. The SeaWinds-NOAA spectra lie above the other spectra for scales from 800 km downward. This is most likely mainly caused by spatially correlated ambiguity removal errors introduced by DIRTH.

[67] The ASCAT-12.5 product contains more small details than the ASCAT-25 product. This is not only indicated by the spectra, but also by the fact that the buoy error is smaller on the scales resolved by ASCAT-12.5 than on the scales of ASCAT-25. The ASCAT-12.5 error standard deviations are 0.7 ms^{-1} for u and 0.8 ms^{-1} for v; those for the ASCAT-25 product are 0.7 ms^{-1} for both u and v. The amount of small scale variance added in ASCAT-12.5 relative to ASCAT-25 is larger than the increase in error. Noise reduction by 2DVAR and MSS removes some small scale information from the SeaWinds-KNMI product, causing better agreement with the ECMWF model and less agreement with the buoys as compared to the ASCAT-25 product. The SeaWinds-KNMI product has an estimated precision of 0.8 ms^{-1} in u and 0.6 ms^{-1} in v. The SeaWinds-NOAA product has the largest error standard deviations: 1.2 ms^{-1} in u and 1.1 ms^{-1} in v, though these figures must be considered with care due to the large representation error in the SeaWinds-NOAA product. Generally, increase in detail as indicated by more variance in

the tail of the spectrum results in better comparison with buoys and worse comparison with ECMWF, as expected.

[68] The calibration coefficients indicate that the ASCAT products and SeaWinds-KNMI underestimate the wind while SeaWinds-NOAA overestimates it. This holds averaged over all wind speeds, scatterometer nodes, and geographical zones as well as the assumptions involved in triple collocation.

[69] The encouraging results for the 12.5-km box-averaged ASCAT winds indicate that ASCAT products at further enhanced resolution may be useful not only near the coast but also over the open ocean in cases of large wind gradients, such as in tropical cyclones and other extreme weather.

[70] **Acknowledgments.** The authors thank their colleagues M. Belmonte Rivas, M. Portabella, and J. Verspeek for their interest in this work and stimulating discussions. They acknowledge the help of ECMWF, in particular J. Bidlot for his assistance with buoy data retrieval and quality control. This work has been funded by EUMETSAT in the context of the NWP SAF and OSI SAF parts of the SAF network.

References

Bidlot, J., D. Holmes, P. Wittmann, R. Lalbeharry, and H. Chen (2002), Intercomparison of the performance of operational ocean wave forecasting systems with buoy data, *Weather Forecast.*, *17*, 287–310, doi:10.1175/1520-0434(2002)017<0287:IOTPOO>2.0.CO;2.

Brennan, M. J., C. C. Hennon, and R. D. Knabb (2009), The operational use of QuikSCAT ocean vector winds at the National Hurricane Center, *Weather Forecast.*, *24*, 621–645, doi:10.1175/2008WAF2222188.1.

Chelton, D. B., M. H. Freilich, J. M. Sienkiewitcz, and J. M. Von Ahn (2006), On the use of QuikSCAT scatterometer measurements of surface winds for marine weather prediction, *Mon. Weather Rev.*, *134*, 2055–2071, doi:10.1175/MWR3179.1.

Errico, R. M. (1985), Spectra computed from a limited area grid, *Mon. Weather Rev.*, *113*, 1554–1562, doi:10.1175/1520-0493(1985)113<1554:SCFALA>2.0.CO;2.

Figa-Saldaña, J., J. J.W. Wilson, E. Attema, R. Gelsthorpe, M. R. Drinkwater, and A. Stoffelen (2002), The advanced scatterometer (ASCAT) on the meteorological operational (MetOp) platform: A follow on for the European wind scatterometers, *Can. J. Remote Sens.*, *28*(3), 404–412, doi:10.5589/m02-035.

Frehlich, R., and R. Sharman (2008), The use of structure functions and spectra from numerical model output to determine effective model resolution, *Mon. Weather Rev.*, *136*, 1537–1553, doi:10.1175/2007MWR2250.1.

Freilich, M. H., and D. B. Chelton (1986), Wavenumber spectra of Pacific winds measured by the SeaSat scatterometer, *J. Phys. Oceanogr.*, *16*, 741–757, doi:10.1175/1520-0485(1986)016<0741:WSOPWM>2.0.CO;2.

Hersbach, H., and P. Janssen (2007), Operational assimilation of surface wind data from the MetOp ASCAT scatterometer at ECMWF, *ECMWF Newsl.*, *113*, 6–8.

Hersbach, H., A. Stoffelen, and S. de Haan (2007), An improved C-band scatterometer ocean geophysical model function: CMOD5, *J. Geophys. Res.*, *112*, C03006, doi:10.1029/2006JC003743.

Janssen, P. A. E. M., S. Abdalla, H. Hersbach, and J.-R. Bidlot (2007), Error estimates of buoy, satellite, and model wave height data, *J. Atmos. Oceanic Technol.*, *24*, 1665–1677, doi:10.1175/JTECH2069.1.

Milliff, R. F. (2004), Comparing the kinetic energy vs. wavenumber in surface wind fields from ECMWF analyses and the NASA QuikSCAT scatterometer, *Contract EVK3-CT-2002-00075*, Ist. Na. di Geofis. e Vulcanol., Rome.

Nastrom, G. D., and K. S. Gage (1985), A climatology of atmospheric wave number spectra of wind and temperature observed by commercial aircraft, *J. Atmos. Sci.*, *42*, 950–960, doi:10.1175/1520-0469(1985)042<0950:ACOAWS>2.0.CO;2.

Nastrom, G. D., K. S. Gage, and W. H. Jasperson (1984), Kinetic energy spectrum of large- and mesoscale processes, *Nature*, *310*, 36–38, doi:10.1038/310036a0.

Patoux, J., and R. A. Brown (2001), Spectral analysis of QuikSCAT surface winds and two-dimensional turbulence, *J. Geophys. Res.*, *106*(D20), 23,995–24,005, doi:10.1029/2000JD000027.

Percival, D. B., and A. T. Walden (1993), *Spectral Analysis for Physical Applications*, Cambridge Univ. Press, Cambridge, U. K., doi:10.1017/CBO9780511622762.

Portabella, M., and A. Stoffelen (2002a), A comparison of KNMI quality control and JPL rain flag for SeaWinds, *Can. J. Remote Sens.*, *28*(3), 424–430, doi:10.5589/m02-040.

Portabella, M., and A. Stoffelen (2002b), Characterization of residual information for SeaWinds quality control, *IEEE Trans. Geosci. Remote Sens.*, *40*, 2747–2759, doi:10.1109/TGRS.2002.807750.

Portabella, M., and A. Stoffelen (2004), A probabilistic approach for SeaWinds data assimilation, *Q. J. R. Meteorol. Soc.*, *130*(596), 127–152, doi:10.1256/qj.02.205.

Portabella, M., and A. Stoffelen (2006), Scatterometer backscatter uncertainty due to wind variability, *IEEE Trans. Geosci. Remote Sens.*, *44*, 3356–3362, doi:10.1109/TGRS.2006.877952.

Portabella, M., and A. Stoffelen (2009), On scatterometer ocean stress, *J. Atmos. Oceanic Technol.*, *26*, 368–382, doi:10.1175/2008JTECHO578.1.

Press, W. H., B. P. Flannery, S. A. Teukolsky, and W. T. Vetterling (1988), *Numerical Recipes*, Cambridge Univ. Press, Cambridge, U. K.

Sienkiewicz, J., M. J. Brennan, R. Knabb, P. S. Chang, H. Cobb, Z. J. Jelenak, K. A. Ahmad, S. Soisuvarn, D. Kosier, and G. Bancroft (2010), Impact of the loss of QuikSCAT on NOAA MWS marine warning and forecast operations, paper presented at First International Ocean Vector Winds Science Team Meeting, Barcelona, Spain, 18–20 May. [Available at http://coaps.fsu.edu/scatterometry/meeting/past.php#2010_may.]

Stiles, B. W., B. D. Pollard, and R. S. Dunbar (2002), Direction interval retrieval with thresholded nudging: A method for improving the accuracy of QuikSCAT winds, *IEEE Trans. Geosci. Remote Sens.*, *40*, 79–89, doi:10.1109/36.981351.

Stoffelen, A. (1998), Toward the true near-surface wind speed: Error modeling and calibration using triple collocation. *J. Geophys. Res.*, *103*(C4), 7755–7766, doi:10.1029/97JC03180.

Stoffelen, A., and D. Anderson (1997), Ambiguity removal and assimilation of scatterometer data, *Q. J. R. Meteorol. Soc.*, *123*, 491–518, doi:10.1002/qj.49712353812.

Stoffelen, A., and M. Portabella (2006), On Bayesian scatterometer wind inversion, *IEEE Trans. Geosci. Remote Sens.*, *44*(6), 1523–1533, doi:10.1109/TGRS.2005.862502.

Tsai, W.-T., M. Spencer, C. Wu, C. Winn, and K. Kellogg (2000), SeaWinds on QuikSCAT: Sensor description and mission overview, in *Geoscience and Remote Sensing Symposium, 2000*, vol. 3, pp. 1021–1023, Inst. of Electr. and Electron. Eng., New York, doi:10.1109/IGARSS.2000.858008.

Vogelzang, J., A. Stoffelen, A. Verhoef, J. de Vries, and H. Bonekamp (2009), Validation of two-dimensional variational ambiguity removal on SeaWinds scatterometer data, *J. Atmos. Oceanic Technol.*, *26*, 1229–1245, doi:10.1175/2008JTECHA1232.1.

Wentz, F. J., and D. K. Smith (1999), A model function for ocean-normalized radar cross section at 14 GHz derived from NSCAT observations, *J. Geophys. Res.*, *104*(C5), 11,499–11,514, doi:10.1029/98JC02148.

J. Figa-Saldaña, EUMETSAT, Eumetsat-Allee 1, Darmstadt, D-64295, Germany.

A. Stoffelen, A. Verhoef, and J. Vogelzang, KNMI, Wilhelminalaan 10, De Bilt, NL-3732 GK, Netherlands. (vogelzan@knmi.nl)